PERIODICO di MINERALOGIA
established in 1930

DIPARTIMENTO DI SCIENZE DELLA TERRA
SAPIENZA UNIVERSITÀ DI ROMA

An International Journal of
Mineralogy, Crystallography, Geochemistry,
Ore Deposits, Petrology, Volcanology
and applied topics on Environment, Archaeometry and Cultural Heritage

Tuhualite revisited: new crystal data and structure refinements on specimens from two localities

Stefano Merlino, Cristian Biagioni *

Department of Earth Sciences, University of Pisa, Via Santa Maria 53, 56126 Pisa, Italy

ARTICLE INFO

Submitted: July 2018
Accepted: September 2018
Available on line: September 2018

* Corresponding author:
cristian.biagioni@unipi.it

DOI: 10.2451/2018PM807

How to cite this article:
Merlino S. and Biagioni C. (2018)
Period. Mineral. 87, 257-267

ABSTRACT

The crystal structure of tuhualite, ideally $Na_2Fe^{2+}{}_2Fe^{3+}{}_2Si_{12}O_{30}$ (Z=4), has been refined on the basis of modern single-crystal X-ray diffraction data using specimens from its type locality (Mayor Island, New Zealand) and from a new occurrence, Pantelleria (Sicily, Italy). Tuhualite is orthorhombic, space group *Cmca*, with unit-cell parameters (Mayor Island/Pantelleria) *a*=14.3285(8)/14.3786(4), *b*=17.2837(10)/17.2098(5), *c*=10.1202(6)/10.0991(3) Å, *V*=2506.3(3)/2499.05(12) Å^3. The crystal structures of both specimens have been refined down to R_1 = 0.0506 [on the basis of 1504 reflections with $F_o>4\sigma(F_o)$] and 0.0240 [on the basis of 2280 reflections with $F_o>4\sigma(F_o)$] for the specimens from Mayor Island and Pantelleria, respectively. The main features of the crystal structure of tuhualite as well as the "anomalous" distribution of Fe^{2+} and Fe^{3+} cations between the tetrahedrally and octahedrally coordinated sites have been confirmed. Moreover, the occurrence of an additional and partially occupied site within the cavities of the octahedral-tetrahedral framework of tuhualite has been observed in the sample from the type locality, in agreement with the excess of alkaline and alkaline earth metals observed in the available chemical data. New data suggest also the possible occurrence of minor vacancies at the tetrahedrally coordinated site that follows the partial oxidation of ferrous iron to ferric iron and the substitution mechanism $3Fe^{2+}=2Fe^{3+}+\square$. The crystal structure of tuhualite is shown by other natural and synthetic compounds. Among natural phases, tuhualite has isotypic relationships with zektzerite and emeleusite. These three phases form the tuhualite group. The micro-Raman spectrum of tuhualite has been collected and compared with those of the other members of the tuhualite group.

Keywords: tuhualite; crystal structure; Raman spectroscopy; chain silicate; tuhualite group; Mayor Islands; New Zealand; Pantelleria; Italy.

INTRODUCTION

Tuhualite, ideally $Na_2Fe^{2+}{}_2Fe^{3+}{}_2Si_{12}O_{30}$ (Z=4), was found in comendite from the Mayor Island (Tuhua for the local inhabitants), New Zealand (Marshall, 1932, 1936). It remained for a long time the only known locality for this rare mineral, before the new recent findings by Andreeva (2016) in the peralkaline granite of the Khaldzan Buregtey Massif, Mongolia, and by Bagiński et al. (2018) in a peralkaline rhyolitic ignimbrite from Pantelleria, Sicily, Italy.

The physical properties, crystal morphology, X-ray powder pattern, and X-ray crystallography of tuhualite, including references to its petrogenesis in the locality of the first finding, have been presented by Hutton (1956) who, on the basis of an analysis of purified material, suggested the following empirical unit cell (*a*=14.31, *b*=17.28, *c*=10.11 Å; space group *Cmca* or *C*2*ca*) content: $H_9(Na,K,Mn)_{12}Fe^{2+}{}_6(Fe^{3+},Al,Mg,Ti)_9(Si_3O_{18})_{15}$. Later on, three microprobe analyses of tuhualite were presented by Nicholls and Carmichael (1969), from which, by assuming

the H_2O content and the ratio of Fe^{3+} to Fe^{2+}, the much simpler ideal formula $(Na,K)_2Fe^{2+}{}_2Fe^{3+}{}_2Si_{12}O_{30}\cdot H_2O$, with four such formulas in the unit cell, could be inferred by Merlino (1969), who carried on the structural study of tuhualite on a specimen kindly borrowed to him by C.O. Hutton.

The structural study was carried on with intensity data collected through integrated Buerger precession photographs [three layers with **a** as precession axis (h=0, 1, 2); the zero layer with **c** as precession axis] with Zr filtered Mo $K\alpha$ radiation. The structure was solved, assuming space group *Cmca*, by examination of the Patterson projection along [100], coupled with the observation of the cell relationships with osumilite $(K,Na)(Mg,Fe^{2+})_2(Al,Fe^{3+})_3(Si,Al)_{12}O_{30}\cdot H_2O$ (a=10.155, c=14.284 Å; space group *P*6/*mmc*) (Brown and Gibbs, 1969).

The structure solution (Merlino, 1969) revealed a new structure-type among the chain silicates, structure-type characterized by six-repeat double chains of SiO_4 tetrahedra. The chains are winding and running along **c**, linking together four chains of edge-sharing iron-centered polyhedra, presenting alternating tetrahedra occupied by Fe^{2+} cations and octahedra occupied by Fe^{3+} cations. These last polyhedral chains, in turn, connect four double chains of SiO_4 tetrahedra by corner-sharing. The sodium cations (with minor K^+ substitution) are placed in the open channels paralleling **a**, with an irregular six-fold coordination. As regards the possible H_2O content, no indications for hydroxyl anions and no clear maxima attributable to H_2O groups have been found during the structural study by Merlino (1969). However, the analytical results by Hutton (1956) [H_2O 1.61 wt%], supported by a new unpublished determination of 1.45 wt% of H_2O (Hutton, 1969: personal communication to S. Merlino), induced the author to propose the ideal formula given above, assuming that 'the water molecule should be randomly distributed' in the structural channels (Merlino, 1969).

The spectroscopic study of tuhualite by Taran and Rossmann (2001) definitely ruled out any H_2O content in the mineral as 'no absorption bands caused by H_2O or OH stretching vibrations have been observed in the 3000 to 4000 cm^{-1} range'. Moreover, the study confirmed the unusual distribution of Fe^{3+} and Fe^{2+} cations among octahedrally and tetrahedrally coordinated sites, respectively.

With the recent findings of tuhualite by Andreeva (2016) and Bagiński et al. (2018) new analytical data have been provided. In particular a set of representative compositions of tuhualite from Pantelleria presented by Bagiński et al. (2018; Table 2) pointed to the formula $Na_2Fe^{3+}{}_2(Fe^{2+},Mn,Zn,Mg)_2Si_{12}O_{30}$, with very minor substitution of Na^+ by K^+ cations.

As the structure of tuhualite was determined with a limited number of reflections, collected with old photographic methods, we deemed useful to take advantage from the availability of the tuhualite specimens from the type locality as well as that from Pantelleria for proceeding to new structural refinements with data collected with modern instruments, with the aim to obtain more precise structural data and compare the crystal chemistry of the two occurrences.

EXPERIMENTAL

Sample description

Two specimens of tuhualite from the Mayor Island (New Zealand) and from Pantelleria, Sicily (Italy) were available. The former was represented by euhedral to subhedral violet crystals, whereas the latter was represented by a fragment of the polished slab of the tuhualite-bearing ignimbrite shown in the Figure 2 of the paper by Bagiński et al. (2018).

X-ray Crystallography

Tuhualite was preliminary identified through X-ray powder diffraction, using a 114.6 mm Gandolfi camera with Ni-filtered Cu $K\alpha$ radiation. The observed pattern for the sample from Pantelleria is given in Table 1 and agrees with that reported by Hutton (1956) for tuhualite from Mayor Island and with that calculated using the software *PowderCell* (Kraus and Nolze, 1996) on the basis of the structural model described below Intensity data were collected for both samples using a Bruker Smart Breeze diffractometer operating at 50 kV and 30 mA and equipped with an air-cooled CCD detector. Graphite-monochromatized Mo $K\alpha$ radiation was used. The detector-to-crystal working distance was set to 50 mm.

Intensity data were integrated and corrected for Lorentz, polarization, background effects, and absorption using the package of software *Apex*3 (Bruker AXS Inc. 2016). The crystal structures were refined, using *Shelxl*-2014 (Sheldrick, 2015), starting from the atomic coordinates given by Merlino (1969). Scattering curves for neutral atoms were taken from the *International Tables for Crystallography* (Wilson, 1992). Details of data collection and crystal structure refinement are reported in Table 2. Table 3 reports atomic coordinates, site occupancies, and equivalent isotropic displacement parameters. Selected bond distances for cations are shown in Table 4.

Tuhualite from Mayor Island

A total of 744 frames were collected using ω scan mode, with an exposure time of 25 seconds per frame. The statistical tests on the distribution of $|E|$ values ($|E^2-1|$ =0.891) points to the centrosymmetric nature of tuhualite

Table 1. X-ray powder diffraction data for tuhualite from Pantelleria, compared with that calculated using the software *PowderCell* 2.3 (Kraus and Nolze, 1996) on the basis of the structural model given in Table 3. Only reflections with $I_{calc} \geq 10$ are reported, if not observed. Observed intensities are visually estimated (vs = very strong; s = strong; ms = medium-strong; m = medium; mw = medium-weak; w = weak; vw = very weak; vvw = very very weak).

This work		Hutton 1956		Calculated, this work			This work		Hutton 1956		Calculated, this work		
I_{obs}	d_{obs}	I_{obs}	d_{obs}	I_{calc}	d_{calc}	*h k l*	I_{obs}	d_{obs}	I_{obs}	d_{obs}	I_{calc}	d_{calc}	*h k l*
mw	8.4	s	8.62	29	8.60	0 2 0	-	-	vw	2.362	7	2.356	2 6 2
m	7.2	vs	7.16	100	7.19	2 0 0	w	2.288	-	-	2	2.296	2 2 4
mw	5.52	s	5.515	36	5.517	2 2 0	m	2.186	s	2.184	10	2.189	4 6 1
-	-	vvw	5.34	-	-	-					14	2.183	0 6 3
vw	5.03	w	5.04	15	5.050	0 0 2	w	2.136	vw	2.147	4	2.151	3 5 3
m	4.85	s	4.85	57	4.842	2 2 1					5	2.134	4 4 3
vw	4.58	vw	4.57	5	4.592	1 1 2	w	2.082	vvw	2.078	3	2.084	2 4 4
mw	4.34	s	4.35	18	4.355	0 2 2	w	2.051	vvw	2.053	4	2.049	4 6 2
-	-	s	4.315	15	4.302	0 4 0	mw	2.010	w	2.002	11	2.009	4 2 4
w	4.12	vw	4.115	15	4.132	2 0 2	w	1.965	w	1.974	5	1.979	0 8 2
vw	3.96	w	3.96	9	3.958	0 4 1					3	1.966	0 2 5
m	3.714	s	3.71	40	3.725	2 2 2	w	1.935	vvw	1.937	6	1.934	6 4 2
-	-	m	3.67	15	3.665	1 3 2	vw	1.912			2	1.904	2 8 2
mw	3.582	m	3.58	16	3.595	4 0 0	mw	1.887	vvw	1.887	6	1.889	1 3 5
mw	3.456	s	3.47	36	3.467	2 4 1					4	1.886	5 1 4
mw	3.313	m	3.31	15	3.317	4 2 0	-	-	vw	1.86	6	1.863	1 9 1
-	-	m	3.285	1	3.275	0 4 2	w	1.847	vw	1.839	4	1.846	5 5 3
m	3.222	m	3.22	29	3.220	1 1 3					5	1.838	5 7 1
-	-	s	3.18	31	3.177	1 5 1	mw	1.801	w	1.789	14	1.797	8 0 0
ms	3.156	m	3.14	38	3.151	4 2 1	w	1.775	vvw	1.767	4	1.778	6 4 3
m	2.977	m	2.97	34	2.980	2 4 2	s	1.732	s	1.726	14	1.738	6 0 4
w	2.922	w	2.926	13	2.928	4 0 2					21	1.728	6 6 2
vw	2.865	vw	2.87	11	2.874	2 2 3	vw	1.681			1	1.683	0 0 6
s	2.772	s	2.766	49	2.772	4 2 2	vw	1.668	vvw	1.669	5	1.673	2 10 0
-	-	vvw	2.75	14	2.759	4 4 0			vvw	1.653	2	1.652	2 10 1
m	2.658	m	2.657	25	2.661	4 4 1	w	1.616			3	1.619	4 8 3
vw	2.567	-	-	1	2.576	2 6 1			vw	1.550	3	1.552	1 7 5
m	2.518	vw	2.522	18	2.525	0 0 4	mw	1.529	vw	1.535	3	1.537	1 11 1
mw	2.496	m	2.490	23	2.494	0 6 2					2	1.524	4 0 6
mw	2.420	w	2.416	13	2.421	4 4 2	w	1.500	vvw	1.501	2	1.504	1 5 6
mw	2.368	vvw	2.378	4	2.382	2 0 4					3	1.501	4 6 5

and the examination of the systematic absences indicates the space group *Cmca*.

After several cycles of isotropic refinement, the R_1 factor converged to 0.078, thus confirming the correctness of the structural model. The site occupancy factor (s.o.f.) at the *Fe*(1) and *Fe*(2) sites was modeled using the scattering curve of Fe *vs* □, whereas the *Na* site was found to be fully occupied by Na, and its s.o.f. was fixed to 1. After the introduction of anisotropic displacement parameters for cations, the R_1 factor converged to 0.066. The difference-Fourier map revealed the occurrence of a maximum at (0, ~0.43, ~0.25). Adding this maximum and refining its s.o.f. using the curve of K *vs* □, the refinement converged to R_1=0.055. Finally, an anisotropic model for all the atom positions converged to 0.0506 for 1504 reflections with $F_o > 4\sigma(F_o)$ and 124 refined parameters.

Table 2. Crystal data and summary of parameters describing data collections and refinements for tuhualite samples.

Crystal data	Mayor Island	Pantelleria
Crystal size (mm^3)	0.090×0.090×0.060	0.125×0.100×0.070
Cell setting, space group	Orthorhombic, *Cmca*	
a (Å)	14.3285(8)	14.3786(4)
b (Å)	17.2837(10)	17.2098(5)
c (Å)	10.1202(6)	10.0991(3)
V ($Å^3$)	2506.3(3)	2499.05(12)
Z	4	
Data collection and refinement		
Radiation, wavelength (Å)	Mo *Kα*, λ = 0.71073	
Temperature (K)	293	
$2\theta_{max}$ (°)	60.06	70.02
Measured reflections	9781	13876
Unique reflections	1901	2636
Reflections with $F_o > 4\sigma$ (F_o)	1504	2280
R_{int}	0.0519	0.0238
Rσ	0.0429	0.0224
Range of h, k, l	-19 ≤*h*≤ 20 -21 ≤ *k* ≤ 24 -14 ≤ *l* ≤ 12	-22 ≤ *h* ≤ 19 -16 ≤ *k* ≤ 27 -16 ≤ *l* ≤ 16
R [$F_o > 4\sigma$ (F_o)]	0.0506	0.0240
R (all data)	0.0739	0.0336
w*R* (on F^2)	0.1523	0.0647
GooF	1.214	1.062
Number of least-square parameters	124	118
Maximun and minimum residuals (*e*/$Å^3$)	1.01 [at 0.72 Å from O(9)] -1.67 [at 1.84 Å from O(3)]	0.84 [at 2.30 Å from O(9)] -0.53 [at 0.66 Å from *Na*]

Tuhualite from Pantelleria

A total of 1020 frames were collected using φ and ω scan modes, with an exposure time of 25 seconds per frame.

After several cycles of isotropic refinement, carried in the space group *Cmca*, the R_1 factor converged to 0.058, thus confirming the correctness of the structural model. The site occupancy factor (s.o.f.) at the *Fe*(1) and *Fe*(2) sites was modeled using the scattering curve of Fe *vs* □; moreover, the s.o.f. at *Na* site was modeled using the curves Na *vs* K. The refinement indicated a full-occupancy by Fe at *Fe*(2) and consequently the s.o.f. at this site was fixed to 1. On the contrary, the s.o.f. at *Fe*(1) and *Na* sites were refined. After the introduction of anisotropic displacement parameters for cations, the R_1 factor converged to 0.034. An anisotropic model for all the atom positions converged to 0.0240 for 2280 reflections with $F_o > 4\sigma(F_o)$ and 117 refined parameters.

Micro-Raman spectroscopy

Unpolarized micro-Raman spectra were collected on unpolished samples of tuhualite from Pantelleria in nearly backscattered geometry with a Jobin-Yvon Horiba XploRA Plus apparatus, equipped with a motorized *x*-*y* stage and an Olympus BX41 microscope with a 10× objective lens. The Raman spectra were excited using a 532 nm line of a solid-state laser. The minimum lateral and depth resolution was set to a few μm. The system was calibrated using the 520.6 cm^{-1} Raman band of silicon before each experimental session. Spectra were collected from 200 to 4000 cm^{-1} through multiple acquisitions with single counting times of 60 s. Backscattered radiation was analyzed with a 1200 mm^{-1} grating monochromator.

DISCUSSION

Crystal structure description

In the conventional classification of silicates, tuhualite

Table 3. Atomic coordinates, site occupation factors (s.o.f.), and equivalent isotropic displacement parameters (Å^2) for tuhualite.

Site	s.o.f.	*x*	*y*	*z*	*U*eq
Mayor Island (New Zealand)					
Fe(1)	$Fe_{0.96(1)}$	0.24693(6)	0.0	0.0	0.0080(3)
Fe(2)	$Fe_{0.96(1)}$	¼	-0.09415(5)	¼	0.0036(3)
Na	$Na_{1.00}$	¼	0.2112(2)	¼	0.0321(9)
K	$K_{0.14(1)}$	0	0.4127(7)	0.2530(11)	0.024(4)
Si(1)	$Si_{1.00}$	0.39057(8)	0.13197(7)	0.01334(12)	0.0061(3)
Si(2)	$Si_{1.00}$	0.38975(8)	0.07147(7)	0.30542(13)	0.0061(3)
Si(3)	$Si_{1.00}$	0.39006(8)	0.18996(7)	0.54169(13)	0.0061(3)
O(1)	$O_{1.00}$	0.3688(3)	0.2225(2)	-0.0084(4)	0.0170(8)
O(2)	$O_{1.00}$	0.3292(2)	0.0795(2)	-0.0829(3)	0.0092(6)
O(3)	$O_{1.00}$	0.3614(2)	0.1120(2)	0.1657(3)	0.0137(7)
O(4)	$O_{1.00}$	0.3302(2)	-0.0045(2)	0.3363(3)	0.0091(6)
O(5)	$O_{1.00}$	0.3626(2)	0.1364(2)	0.4146(3)	0.0135(7)
O(6)	$O_{1.00}$	0.3294(2)	0.1723(2)	0.6681(3)	0.0108(7)
O(7)		½	0.1150(3)	-0.0060(5)	0.0189(12)
O(8)	$O_{1.00}$	½	0.0546(3)	0.3074(5)	0.0148(10)
O(9)	$O_{1.00}$	½	0.1810(3)	0.5708(6)	0.0196(12)
Pantelleria (Italy)					
Fe(1)	$Fe_{0.96(1)}$	0.24664(2)	0.0	0.0	0.0124(1)
Fe(2)	$Fe_{1.00}$	¼	-0.09504(2)	¼	0.0077(1)
Na	$Na_{0.97(1)}K_{0.03(1)}$	¼	0.21862(6)	¼	0.0310(6)
Si(1)	$Si_{1.00}$	0.39162(2)	0.13206(2)	0.01148(4)	0.0079(1)
Si(2)	$Si_{1.00}$	0.39045(2)	0.06959(2)	0.30401(4)	0.0080(1)
Si(3)	$Si_{1.00}$	0.39109(2)	0.18841(2)	0.54286(4)	0.0077(1)
O(1)	$O_{1.00}$	0.37189(8)	0.22334(6)	-0.00969(12)	0.0166(2)
O(2)	$O_{1.00}$	0.32791(7)	0.08065(6)	-0.08405(10)	0.0110(2)
O(3)	$O_{1.00}$	0.36213(7)	0.11137(7)	0.16461(11)	0.0155(2)
O(4)	$O_{1.00}$	0.32918(7)	-0.00576(6)	0.33444(11)	0.0119(2)
O(5)	$O_{1.00}$	0.36353(8)	0.13415(7)	0.41610(11)	0.0154(2)
O(6)	$O_{1.00}$	0.32769(7)	0.17270(6)	0.66831(11)	0.0127(2)
O(7)	$O_{1.00}$	½	0.11260(11)	-0.00827(17)	0.0178(3)
O(8)	$O_{1.00}$	½	0.05164(10)	0.30577(18)	0.0174(3)
O(9)	$O_{1.00}$	½	0.17802(11)	0.57479(18)	0.01882(3)

takes its place among the chain silicates, in a subgroup characterized by six-repeat double chains of SiO_4 tetrahedra (Figure 1), *sechser-doppelketten* according to the classification by Liebau (1972). It seems interesting to recall that Zoltai (1960) proposed a classification of tetrahedral structures based on the degree of polymerization of the tetrahedral units, irrespective of their chemical nature. With Fe^{2+}, more precisely (Fe^{2+}, Mn, Zn, Mg), among the linked tetrahedra, tuhualite, as well as any other compound with tuhualite-like structure-type (see below), displays a framework-like structure, with a ratio between the number of tetrahedral cations and oxygen anions of 14:30, corresponding to an interrupted framework, with interruption in only four out of 30 oxygen anions [O(6) atoms, in the present structural study, as indicated in Figure 1].

The SiO_4 tetrahedra are quite regular with average bond distances 1.612 Å, 1.614 Å, 1.610 Å (sample from

Table 4. Selected bond distances (in Å) in tuhualite.

		Mayor Island	Pantelleria			Mayor Island	Pantelleria			Mayor Island	Pantelleria
Fe(1)	–O(4)	1.993(3)×2	1.9985(11)×2	*Si*(1)	–O(2)	1.595(3)	1.5977(11)	*Na*	–O(6)	2.318(4)×2	2.3296(14) ×2
	–O(2)	1.996(3)×2	2.0032(10)×2		–O(7)	1.607(2)	1.6063(6)		–O(3)	2.614(4)×2	2.5979(14) ×2
					–O(1)	1.611(4)	1.6106(12)		–O(5)	2.743(4)×2	2.7553(14) ×2
Fe(2)	–O(6)	1.951(3)×2	1.9985(11)×2		–O(3)	1.634(4)	1.6426(11)		–O(1)	3.120(4)×2	3.1553(12) ×2
	–O(2)	2.053(3)×2	2.0032(10)×2						–O(1)	3.134(4)×2	3.1559 (12) ×2
	–O(4)	2.117(3)×2		*Si*(2)	–O(4)	1.597(3)	1.5976(11)				
					–O(8)	1.607(2)	1.6053(5)	*K*	–O(9)	2.408(13)	-
					–O(3)	1.623(4)	1.6324(11)		–O(8)	2.513(13)	-
					–O(5)	1.630(4)	1.6328(12)		–O(7)	2.545(13)	-
									–O(4)	2.945(8)×2	-
				Si(3)	–O(6)	1.576(3)	1.5841(11)		–O(6)	2.962(8)×2	-
					–O(9)	1.610(2)	1.6087(5)		–O(2)	2.994(7)×2	-
					–O(1)	1.624(4)	1.6323(12)				
					–O(5)	1.632(4)	1.6332(11)				

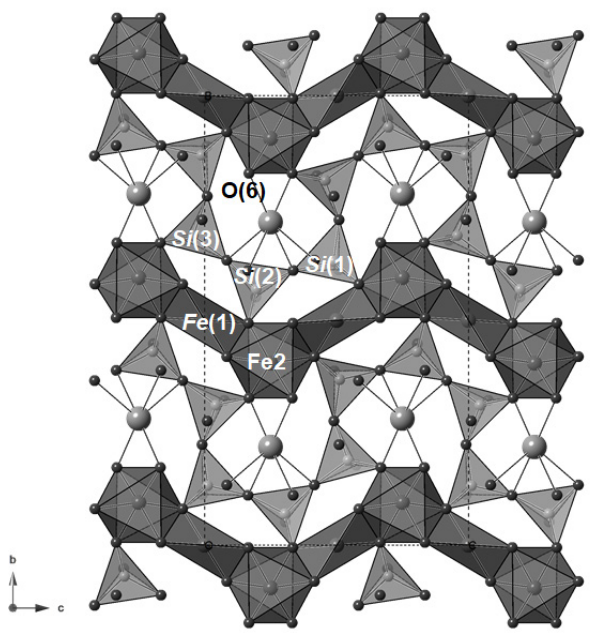

Figure 1. Crystal structure of tuhualite as seen down **a**. The additional *K* site of sample from the type locality is not shown.

the type locality) and 1.615 Å, 1.617 Å, 1.615 Å (sample from Pantelleria) for the tetrahedra centered by *Si*(1), *Si*(2) and *Si*(3), respectively. Such distances suggested a pure Si occupancy of these sites. On the contrary the tetrahedron around *Fe*(1) is highly distorted, and may be more correctly denoted as a bisphenoid (Figure 2: in the Figure the O O' atoms are related by a twofold axis parallel to **a** and passing through the *Fe*(1) atom). The distortion of the *Fe*(1)-centered tetrahedron can be appreciated taking into account the quadratic elongation and the variance of bond angles calculated according to Robinson et al. (1971). Indeed, in the sample from Pantelleria, the mean quadratic elongation λ and the bond angles variance σ^2 are 1.1352 and 486.02, respectively, to be compared with the values obtained for the quite regular SiO_4 tetrahedra, with λ ranging between 1.0009 [*Si*(1)] and 1.0030 [*Si*(2)] and σ^2 values between 3.912 for the less distorted *Si*(1)-centered tetrahedron and 12.167 for the more distorted *Si*(2)-centered tetrahedron. The *Fe*(2)-centered octahedron is substantially regular. Finally, the sodium cations are irregularly coordinated by six oxygen atoms, with distances ranging from 2.32 to 2.74 Å (sample from the type locality) and 2.33 to 2.76 Å (sample from Pantelleria).

A peculiar feature in the crystal structure of tuhualite was the 'anomalous' distribution of Fe^{3+} and Fe^{2+} cations between the octahedrally and tetrahedrally coordinated sites of the iron polyhedral chains running along **c**. The actual distribution was determined by Merlino (1969)

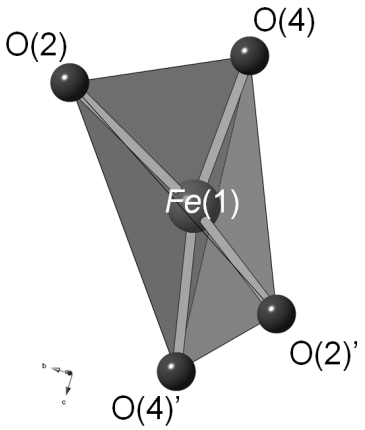

	x	y	z
O(2)	0.3279	0.0806	-0.0840
O(4)	0.1708	0.0058	-0.1656
Fe(1)	0.2466	0	0

O(2) – *Fe*(1) – O(4)'	135.00° (x2)
O(2) – *Fe*(1) – O(4)	85.95° (x2)
O(2) – *Fe*(1) – O(2)'	108.62°
O(4) – *Fe*(1) – O(4)'	113.88°

Figure 2. The distorted tetrahedral coordination of *Fe*(1) and its geometrical features (data based on the refinement of the sample from Pantelleria).

by comparing the calculated bond distances with the experimental ones. We may repeat here that calculation with the new data, which are largely more precise than those obtained by Merlino (1969) for the structure of tuhualite from Mayor Island. For the calculated bond distances, we use the ionic radii presented by Shannon (1976): $^{III}O^{2-}$ (1.36 Å), $^{VI}Fe^{2+}$ (0.78 Å), $^{IV}Fe^{2+}$ (0.64 Å), $^{VI}Fe^{3+}$ (0.645 Å), $^{IV}Fe^{3+}$ (0.49 Å).

Therefore, the calculated distances for the two possible options are the following:

$^{VI}Fe^{3+}$–$^{III}O^{2-}$=2.005 Å $^{IV}Fe^{2+}$–$^{III}O^{2-}$=2.00 Å

$^{IV}Fe^{3+}$–$^{III}O^{2-}$= 1.85 Å $^{VI}Fe^{2+}$–$^{III}O^{2-}$=2.14 Å

As the mean bond distance *Fe*(1)–O is 1.994 Å (type locality) and 2.001 Å (Pantelleria) and the mean bond distance *Fe*(2)–O is 2.040 Å (type locality) and 2.017 Å (Pantelleria), the best match between calculated and determined distances is obtained with Fe^{2+} and Fe^{3+} in tetrahedral and octahedral coordination, respectively. This distribution, which (as previously mentioned) has been validated by the spectroscopic study by Taran and Rossmann (2001), is confirmed by the bond valence balance (Table 5), calculated using the bond parameters of Brese and O'Keeffe (1991).

Sodium and minor K is hosted in cavities of the octahedral-tetrahedral framework having a six-fold coordination; four additional longer bonds complete the coordination sphere. Chemical analyses of tuhualite available in literature (see below) usually show an excess of alkaline and alkaline earth cations. These excess cations find location in the site 8*f* at ~(0, 0.41, 0.26). This site shows acceptable distances from nine oxygen atoms, ranging between ~2.30-2.40 Å and 3.0 Å, and is actually found partially occupied in tuhualite from the type locality (*K* site) and fully occupied in a set of compounds with tuhualite structure-type (see below).

Crystal-chemistry of tuhualite

The results of the crystal structure refinement of tuhualite from the type locality and Pantelleria can be interpreted on the basis of the literature chemical data and given by Hutton (1956), Nicholls and Carmichael (1969), and Bagiński et al. (2018).

Tuhualite from Mayor Island

Four chemical analyses of tuhualite from Mayor Island are available in literature (Hutton, 1959; Nicholls and Carmichael, 1969). Whereas Hutton (1959) determined the amount of FeO and Fe_2O_3, Nicholls and Carmichael (1969) gave the total iron as FeO. Consequently, for the three analyses of these last authors, the Fe^{2+}/Fe^{3+} atomic ratio was recalculated, on the basis of 15 O apfu and a total of six positive charges for the sites *Fe*(1), *Fe*(2), *Na*, and *K*, assuming that Si-centered tetrahedra are occupied by Si^{4+} only, as suggested by crystal structure refinement. The four chemical analyses correspond to the following chemical formulae (given as unit formulae – *Z*=8):

i) $(Na_{1.29}K_{0.21})_{\Sigma 1.50}(Fe^{3+}_{0.89}Al_{0.07}Ti_{0.03})_{\Sigma 0.99}(Fe^{2+}_{0.75}Mg_{0.06}Mn_{0.06}Fe^{3+}_{0.10})_{\Sigma 0.97}Si_{5.85}O_{15}$ (Hutton, 1959),

ii) $(Na_{0.55}K_{0.49}Ca_{0.01})_{\Sigma 1.05}(Fe^{3+}_{0.90}Al_{0.06}Zr_{0.01})_{\Sigma 0.97}(Fe^{2+}_{0.92}Mn_{0.09})_{\Sigma 1.01}Si_6O_{15}$ (sample NZC-4777 Blue var. – Nicholls and Carmichael, 1969);

iii) $(Na_{1.09}K_{0.09}Ca_{0.02})_{\Sigma 1.20}(Fe^{3+}_{0.98}Al_{0.02})_{\Sigma 1.00}(Fe^{2+}_{0.76}Mn_{0.04}Fe^{3+}_{0.05})_{\Sigma 0.85}Si_6O_{15}$ (sample NZC-4777 Violet var. - Nicholls and Carmichael, 1969);

iv) $(Na_{1.08}K_{0.01}Ca_{0.01})_{\Sigma 1.10}(Fe^{3+}_{0.95}Al_{0.01})_{\Sigma 0.96}(Fe^{2+}_{0.84}Mn_{0.13}Mg_{0.01})_{\Sigma 0.98}Si_6O_{18}$ (sample NZC-5 – Nicholls and Carmichael, 1969).

All four analyses revealed an excess of alkaline and alkaline earth cations, ranging from 0.05 to 0.50 apfu,

Table 5. Bond valence sums (in valence unit, *v.u.*) in tuhualite.

Mayor Island

	Fe(1)	*Fe*(2)	*Na*	*K*	*Si*(1)	*Si*(2)	*Si*(3)	Σanions
O(1)			$0.03^{\downarrow\times2}$ $0.03^{\downarrow\times2}$		1.04		1.00	2.10
O(2)	$0.47^{\downarrow\times2}$	$0.43^{\downarrow\times2}$		$0.01^{\downarrow\times2}$	1.08			1.99
O(3)			$0.11\downarrow\times2$		0.97	1.00		2.08
O(4)	$0.48^{\downarrow\times2}$	$0.36^{\downarrow\times2}$		$0.02^{\downarrow\times2}$		1.08		1.94
O(5)			$0.08^{\downarrow\times2}$			0.98	0.98	2.04
O(6)		$0.57^{\downarrow\times2}$	$0.25^{\downarrow\times2}$	$0.01^{\downarrow\times2}$			1.14	1.97
O(7)				0.05	$^{2x\rightarrow}1.05$			2.15
O(8)				0.05		$^{2x\rightarrow}1.05$		2.15
O(9)				0.07			$^{2x\rightarrow}1.04$	2.15
Σcations	1.90	2.72	1.00	0.25	4.14	4.11	4.16	

Pantelleria

	Fe(1)	*Fe*(2)	*Na*	*Si*(1)	*Si*(2)	*Si*(3)	Σanions
O(1)			$0.02^{\downarrow\times2}$ $0.02^{\downarrow\times2}$	1.04		0.98	2.06
O(2)	$0.46^{\downarrow\times2}$	$0.48^{\downarrow\times2}$		1.07			2.01
O(3)			$0.12^{\downarrow\times2}$	0.95	0.98		2.05
O(4)	$0.47^{\downarrow\times2}$	$0.40^{\downarrow\times2}$			1.07		1.94
O(5)			$0.08^{\downarrow\times2}$		0.98	0.98	2.04
O(6)		$0.63^{\downarrow\times2}$	$0.25^{\downarrow\times2}$			1.11	1.99
O(7)				$^{2x\rightarrow}1.05$			2.10
O(8)					$^{2x\rightarrow}1.05$		2.10
O(9)						$^{2x\rightarrow}1.04$	2.08
Σcations	1.86	3.02	0.98	4.11	4.08	4.11	

Note: left and right superscripts indicates the number of equivalent bonds involving cations and anions, respectively. For sites with mixed occupancy, the bond valences have been weighted.

in agreement with the result of the crystal structure refinement. Indeed, the violet crystal from Mayor Island studied in this work shows the *Na* site fully occupied by Na^+, and an additional site, at (0, 0.413, 0.253) having a site occupancy factor (s.o.f.) $K_{0.14}$. The sum of the observed site scattering at the *Na* and *K* sites is 13.7 electrons per formula unit (epfu), in agreement with the analysis of the violet variety of tuhualite (sample NZC-4777 Violet var.) reported by Nicholls and Carmichael (1969), i.e., 14.1 epfu. This cation excess could be balanced through some vacancies at the *Fe*(1) and *Fe*(2) sites, or through substitution of Fe^{3+} by Fe^{2+}.

The tetrahedrally and octahedrally coordinated sites of tuhualite are occupied by (Fe^{2+}, Mn^{2+}, Mg^{2+}, Fe^{3+}) and (Fe^{3+}, Al), respectively. Bond distances, refined site scattering, and bond-valence sums agrees with such site assignments.

Tuhualite from Pantelleria

The chemical analyses of two prismatic subhedral crystals (Bagiński et al., 2018; crystals 1 and 2 in Table 2), corresponding to the crystal used in the present paper for the data collection, gave the following unit-formulae (Z=8):

Crystal 1 $(Na_{1.08}K_{0.03})_{\Sigma1.11}Fe^{3+}(Fe^{2+}_{0.42}Fe^{3+}_{0.14}Mn_{0.26}Zn_{0.04}Mg_{0.04})_{\Sigma0.90}Si_6O_{15}$

Crystal 2 $(Na_{1.03}K_{0.01})_{\Sigma1.04}Fe^{3+}(Fe^{2+}_{0.66}Fe^{3+}_{0.05}Mn_{0.19}Zn_{0.04}Mg_{0.02})_{\Sigma0.96}Si_6O_{15}$

On the basis of these analytical data we may interpret the results of our refinement. The incomplete occupancy at the *Fe*(1) site (0.95 atoms) may be explained with the presence of a quantity of Fe^{3+} cations in the site, with the consequent substitution of Fe^{2+} (or other divalent cations)

according to the following mechanism:

$3Fe^{2+}=2Fe^{3+}+\square$

In accordance with this interpretation, a higher vacancy is found in crystal 1, which presents a higher content of Fe^{3+} at the site *Fe*(1).

The excess of alkali cations (0.11 in crystal 1, 0.04 in crystal 2) could likely find location in the site 8*f* at (1/2, 0.09, 0.74), corresponding to the 'residual maximum' (0.84 *e*/Å^3) resulting at the end of the refinement process. This site shows acceptable distances from nine oxygen atoms, ranging between ca. 2.30 Å and 3.02 Å.

Related compounds

A number of compounds, both natural and synthetic, display the structure-type of tuhualite (Table 6). They differ one from the other for two aspects:

a) the chemical nature of the cations placed in alternating tetrahedral (site 8*d*) and octahedral (site 8*e*) polyhedra, building up chains running along **c**;

b) the occupancy by Na cations or vacancy of the site 8*f* at (0, ~0.43, ~0.25). The site is occupied when the sum of the charges of the cations in the 8*d* and 8*e* sites of the polyhedral chains is equal to +4; it is empty when that sum is +5.

These considerations indicate that a wide number of compounds with the structure-type of tuhualite may be synthesized or found in nature, provided that the coordination and charge balance requirements are satisfied. Some examples of possible formulations have been listed by Ghose and Wan (1978). Up to now, only three natural phases having the structure-type of tuhualite have been described: tuhualite (Marshall, 1932), zektzerite (Dunn et al., 1977), and emeleusite (Upton et al., 1978). Since these minerals have essentially the same structure and are composed of chemically similar elements, following Mills et al. (2009) they may be ascribed to the tuhualite group.

Micro-Raman spectroscopy

The micro-Raman spectrum of tuhualite (Figure 3) can be divided in two distinct regions, i.e., 200-600 cm^{-1}, and 900-1200 cm^{-1}. The strongest bands are located in the latter region, where Si–O stretching modes occur, in agreement with Raman studies on other chain silicates (e.g., Kieffer, 1980; Apopei and Buzatu, 2010; Buzatu and Buzgar, 2010). The most intense band occurs at 985 cm^{-1} and shows a shoulder at 954 cm^{-1}. Two additional bands occur at 1100 and 1122 cm^{-1}. Bands occurring in the range 200-600 cm^{-1} are likely related both to the bending of Si–O bonds as well as M–O bonds, where M=Na, Fe, and other minor cations. No evidence of the occurrence of O–H bonds occurs in the range 3000-4000 cm^{-1} (not shown), in agreement with Taran and Rossmann (2001).

Figure 3 shows also the Raman spectra of the other natural members of the tuhualite group. The spectra are very similar in the region between 900 and 1200 cm^{-1}, owing to the identical nature of silicate chains. On the contrary, in the region between 200 and 600 cm^{-1}, the spectra of tuhualite and zektzerite are similar (but not identical), whereas significant differences can be observed in the spectrum of emeleusite. Indeed, whereas in tuhualite and zektzerite the additional 8*f* site is empty, or only very partially occupied, in emeleusite sodium is hosted at this position. Since in this region, the M–O modes occur, such differences could be related to this crystal-chemical diversity.

The bands between 600 and 800 cm^{-1} occurring in the

Table 6. Natural and synthetic compounds related to tuhualite.

Compound	Site 8*d*	Site 8*e*	Site 8*f*	Chemical formula[2]	Ref.
Tuhualite	Fe^{2+}	Fe^{3+}	□	$\square NaFe^{2+}Fe^{3+}Si_6O_{15}$	[1]
Emeleusite[1]	Li^+	Fe^{3+}	Na^+	$NaNaLiFe^{3+}Si_6O_{15}$	[2]
Zektzerite	Li^+	Zr4+	□	$\square NaLiZrSi_6O_{15}$	[3]
Synthetic	Mg^{2+}	Mg^{2+}	Na^+	$NaNaMg_2Si_6O_{15}$	[4]
Synthetic	Li^+	Y^{3+}	Na^+	$NaNaLiYSi_6O_{15}$	[5]
Synthetic	Na^+	Y^{3+}	Na^+	β-$NaNaNaYSi_6O_{15}$	[6]
Synthetic	Na^+	Dy^{3+}	Na^+	$NaNaNaDySi_6O_{15}$	[7]

[1] Merlino, 1969; [2] Johnsen et al., 1978; [3] Ghose and Wan, 1978; [4] Cradwick and Taylor, 1972; [5] Gunawardane et al., 1982; [6] Bourguiba and Dogguy, 1994; [7] Ziadi et al., 2004.
[1] A synthetic analogue of emeleusite was prepared and studied by Sandomirski et al. (1975).
[2] Chemical formulae are unit-formulae based on 15 O apfu.

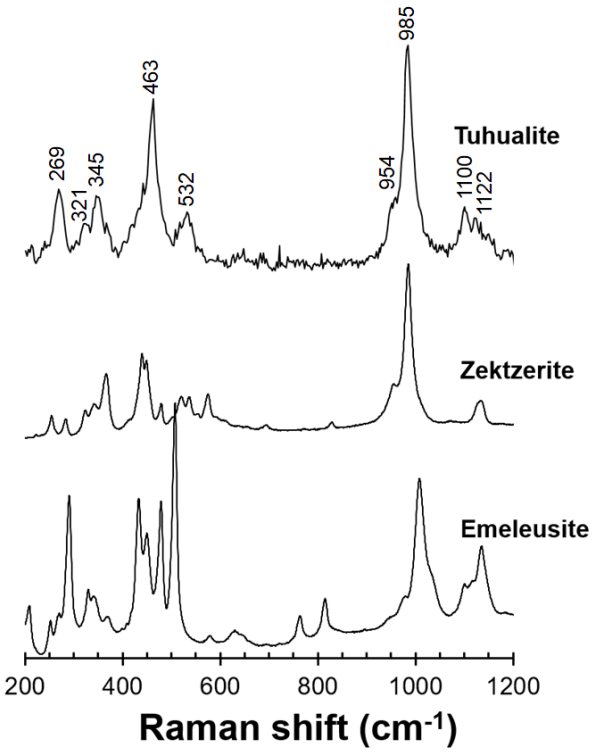

Figure 3. Raman spectra of members of the tuhualite group in the range 200-1200 cm^{-1}. Data for zektzerite and emeleusite are from the RRUFF Project (Lafuente et al., 2015).

spectra of zektzerite and emeleusite, and not observed in tuhualite, are probably related to the bending of Si–O bonds. In tuhualite, only a weak and broad band likely occur at ~645 cm^{-1}.

ACKNOWLEDGEMENTS

We wish to thank Bogusław Bagiński and Marco E. Ciriotti for providing us with the studied specimens from Pantelleria and Mayor Island, respectively. The comments of Ferdinando Bosi and an anonymous reviewer helped us to improve the paper.

REFERENCES

Andreeva I., 2016. Genesis and mechanisms of formation of rare metal peralkaline granites of the Khaldzan Buregtey Massif, Mongolia: evidence from melt inclusions. Petrology 24, 462-476.

Apopei A.I. and Buzgar N., 2010. The Raman study of amphiboles. Analele Ştiinţifice Ale Universităţii "Al. I. Cuza" Iaşi, Geologie 56, 57-83.

Bagiński B., Macdonald R., White J.C., Jeżak L., 2018. Tuhualite in a peralkaline rhyolitic ignimbrite from Pantelleria, Italy. European Journal of Mineralogy 30, 367-373.

Brese N.E., O'Keeffe M., 1991. Bond-valence parameters for solids. Acta Crystallographica B47, 192-197.

Bourguiba N.F. and Dogguy L.S., 1994. Preparation et affinement de la structure d'un silicate a double chaines d'yttrium et de trisodium. Materials Research Bulletin 29, 427-436.

Brown G.E. and Gibbs G.V., 1969. Refinement of the crystal structure of osumilite. American Mineralogist 54, 101-116.

Bruker AXS Inc., 2016. APEX 3. Bruker Advanced X-ray Solutions, Madison, Wisconsin, USA.

Buzatu A. Buzgar N., 2010. The Raman study of single-chain silicates. Analele Ştiinţifice Ale Universităţii "Al. I. Cuza" Iaşi, Geologie 56, 107-125.

Cradwick M.E. and Taylor H.F.W., 1972. The crystal structure of $Na_2Mg_2Si_6O_{15}$. Acta Crystallographica B28, 3583-3587.

Dunn P.J., Rouse R.C., Cannon B., Nelen J.A., 1977. Zektzerite: a new lithium sodium zirconium silicate related to tuhualite and the osumilite group. American Mineralogist 62, 416-420.

Ghose S. and Wan C., 1978. Zektzerite, $NaLiZrSi_6O_{15}$, a silicate with six-tetrahedral-repeat double chains. American Mineralogist 63, 304-310.

Gunawardane R.P., Howie R.A., Glasser F.P., 1982. Structure of Lithium Sodium Yttrium Silicate $Na_2LiYSi_6O_{15}$. Acta Crystallographica B38, 1405-1408.

Hutton C.O., 1956. Re-examination of the mineral tuhualite. Mineralogical Magazine 31, 96-106.

Johnsen O., Nielsen K., Sotofte I., 1978. The crystal structure of emeleusite, a novel example of sechser-doppelkette. Zeitschrift für Kristallographie 147, 297-306.

Kieffer S.W., 1980. Thermodynamics and lattice vibrations of minerals: 4. Application to chain and sheet silicates and orthosilicates. Reviews of Geophysics and Space Physics, 18, 862-886.

Kraus W., Nolze G., 1996. PowderCell – a program for the representation and manipulation of crystal structures and calculation of the resulting X-ray powder patterns. Journal of Applied Crystallography 29, 301-303.

Lafuente B., Downs R.T., Yang H., Stone N., 2015. The power of databases: the RRUFF project. In: Highlights in Mineralogical Crystallography, T. Armbruster and R.M. Danisi, eds. Berlin, Germany, W. De Gruyter, 1-30.

Liebau F., 1972. Crystal chemistry of silicon. In H.K. Wedepohl, Ed., Handbook of Geochemistry, II/3, 14-A-1-14-A-32, Springer-Verlag, Berlin.

Marshall P., 1932. Notes on some volcanic rocks of the North Island of New Zealand. The New Zealand Journal of Science and Technology, 13, 201.

Marshall P., 1936. The mineral tuhualite. Transactions and Proceedings of the New Zealand Institute 66, 330-336.

Merlino S., 1969. Tuhualite crystal structure. Science, 166, 1399-1401.

Mills S.J., Hatert F., Nickel E.H., Ferraris G., 2009. The standardisation of mineral group hierarchies: application to recent nomenclature proposals. European Journal of Mineralogy, 21, 1073-1080.

Nicholls J., Carmichael I.S.E., 1969. Peralkaline acid liquids: a petrological study. Contributions to Mineralogy and Petrology 20, 268-294.

Robinson K., Gibbs G.V., Ribbe P.H., 1971. Quadratic elongation: a quantitative measure of distortion in coordination polyhedral. Science 171, 567-570.

Sandomirski P.A., Simonov M.A., Belov N.B., 1975. Crystal structure of $Na_2LiFe[Si_2O_5]_3$. Dokladi Akademi SSSR, 221, 842-845 (in Russian).

Shannon R.D., 1976. Revised effective ionic radii and systematic studies of interatomic distances in halides and chalcogenides. Acta Crystallographica, A32, 751-767.

Sheldrick G.M., 2015. Crystal structure refinement with SHELXL. Acta Crystallographica C71, 3-8.

Taran M.N. and Rossman, G.R., 2001. Optical spectroscopic study of tuhualite and a re-examination of the beryl, cordierite, and osumilite spectra. American Mineralogist 86, 973-980.

Upton B.G.J., Hill P.G., Johnsen O., Petersen O.V., 1978. Emeleusite, a new LiNaFeIII silicate from south Greenland. Mineralogical Magazine 42, 31-34.

Wilson A.J.C., Ed., 1992. International Tables for Crystallography, Volume C: Mathematical, physical and chemical tables. Kluwer Academic, Dordrecht, NL.

Ziadi A., Hillebrecht H., Thiele G., Elouadi B., 2004. Structure determination of $Na_3DySi_6O_{15}$ and crystal chemistry of zektzerite related compounds. Journal of Solid State Chemistry 177, 4777-4784.

Zoltai T., 1960. Classification of silicates and other minerals with tetrahedral structures. American Mineralogist 45, 960-973.

This work is licensed under a Creative Commons Attribution 4.0 International License CC BY. To view a copy of this license, visit http://creativecommons.org/licenses/by/4.0/